Master of Science in Mechanical Engineering

Soft sensor and gripper for extremely flexible objects

초유연 물체용 소프트 센서와 그리퍼

February 2023

Graduate School of Mechanical Engineering
Seoul National University

Uhsang Ahn

Soft sensor and gripper for extremely flexible objects

Advisor Ho-Young Kim

Submitting a master's thesis of Mechanical Engineering

October 2022

Graduate School of Mechanical Engineering
Seoul National University

Uhsang Ahn

Confirming the master's thesis written by Uhsang Ahn

December 2022

Chair	Hyungmin Park	(Seal)
Vice Chair	Ho-Young Kim	(Seal)
Examiner	Wontae Hwang	(Seal)

Abstract

Automation and smart manufacturing methods have seen widespread adoption in many industries, ranging from automotive manufacturing to unmanned cashiers in the service sector. The garments manufacturing industry, however, remains highly labor intensive, despite increasing global labor costs, primarily due to the difficulties modern robotic manipulators face handling extremely flexible objects, such as fabrics. Here we present a soft gripper that is able to firmly grip single sheets of fabric from a stack without causing damage. The gripper also demonstrates good single sheet separation capabilities. The imperfections in single sheet separation are overcome through embedding soft capacitive sensors which provide information on how many sheets of fabric, if any, are gripped. Theoretical models on the holding force and sensing capabilities are provided, and applications in the garments industry are explored.

Keyword : soft gripper, soft sensor, automation
Student Number : 2019-21912

Table of Contents

Chapter 1. Introduction

Advancement in robotics and artificial intelligence (AI) have shifted towards higher levels of automation in many manufacturing industries. Many automobile factories, for example, have automated a significant portion of the welding process with robotic arms[1], which not only increase productivity but also reduce the risk of human error and health hazards associated with welding.

The garments manufacturing industry, however, remains highly labor-intensive in almost all stages of manufacturing[2]. A key hinderance to automating the garments manufacturing process is the difficulties faced by modern robots when attempting to handle extremely soft, flexible and free-form objects, such as fabrics. Extremely flexible objects, especially fabrics, have the tendency to fold and deform when handled. Thus, it becomes exceptionally difficult to maintain the object's original shape and orientation, even when undergoing simple pick-and-place processes.

There have been many attempts to develop grippers to solve the problem of handling extremely flexible objects such as fabrics. Suctions cups use air flow or suction[3],[4], electrostatic adhesion grippers use a high electric field to induce electrical polarity to generate electrostatic force[5],[6], and needle grippers use needles that pierce fabrics to form an interlocking grip[7],[8]. Current fabric gripping technologies, however, have significant tradeoffs that make the aforementioned fabric grippers unattractive solutions to utilize in widespread garment manufacturing automation technologies. Suction cups, for example, are highly unreliable when attempting to grip porous fabrics. Electrostatic fabric grippers suffer from a long cycle time, as well as a very weak force, which decreases its reliability in a fast-paced manufacturing line. Needle grippers, though reliable and fast, are prone to cause permanent damage to fabrics.

To overcome the aforementioned tradeoffs commercial fabric grippers experience, we present a pneumatically actuated soft gripper that can reliably pinch a single sheet of fabric from a stack. We further demonstrate the soft gripper's applicability to the garments manufacturing industry by embedding soft sensors which allows for controlled pick and place tasks while discerning the number of fabric sheets gripped.

Chapter 2. Design and Fabrication

2.1. Soft gripper design and working principle

The design of the soft gripper is shown in Figure 2.1. The soft gripper comprises two opposing gripping fingers, which measure 13 mm in length, 18 mm in width and 3.5 mm in thickness. The gripping fingers are joined by a thin cavity membrane and cavity walls, creating an airtight cavity. Each gripping finger possesses a notch at the base which acts as a soft hinge. The gripping fingers extend beyond the cavity membrane and are joined at the tips by a thin gripping membrane.

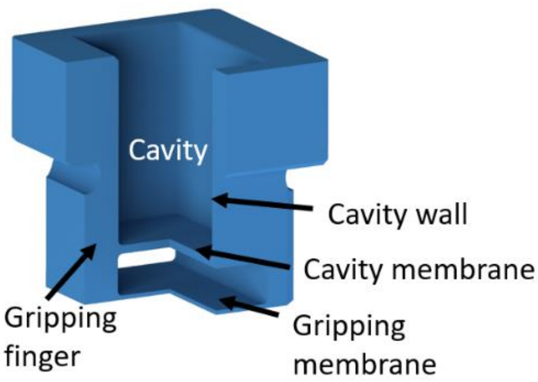

Figure 2.1: Section view schematic of the soft gripper.

Figure 2.2 shows the working principle of the soft gripper. When the pressure inside the cavity is equal to the atmospheric pressure, the gripper remains inactive. However, when the air pressure is dropped below the atmospheric air pressure, the cavity membrane and cavity walls collapse, while the gripping fingers are pulled in towards each other. During this process, the gripping membrane buckles and folds into the gap between the gripping fingers.

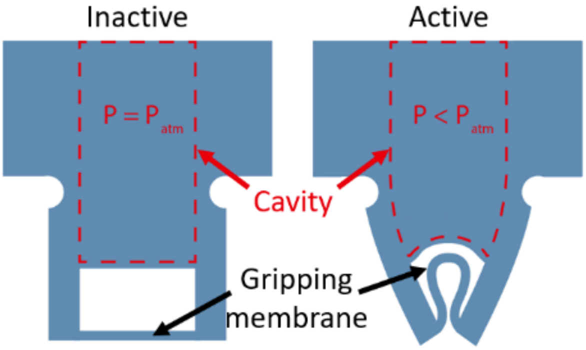

Figure 2.2: Soft gripper working principle.

Depending on the relative position of the soft gripper with the stack of the fabric, the soft gripper employs two distinct modes of gripping. The first mode of gripping -- pinching -- occurs when the edge of the fabric stack is not located between the gripping fingers and is shown in Figure 2.3(a). As the gripper is actuated, the gripping membrane and the sheet of fabric buckles, folding into a loop between the two gripping fingers for a secure grip. The second mode of gripping -- edge lifting -- occurs when the edge of the fabric stack is located between the two gripping fingers, as shown in Figure 2.3(b). As the gripper is actuated, the buckling mechanism of the gripping membrane lifts the edge of one sheet of fabric. This allows the gripper to grip a single sheet of fabric without requiring a fold.

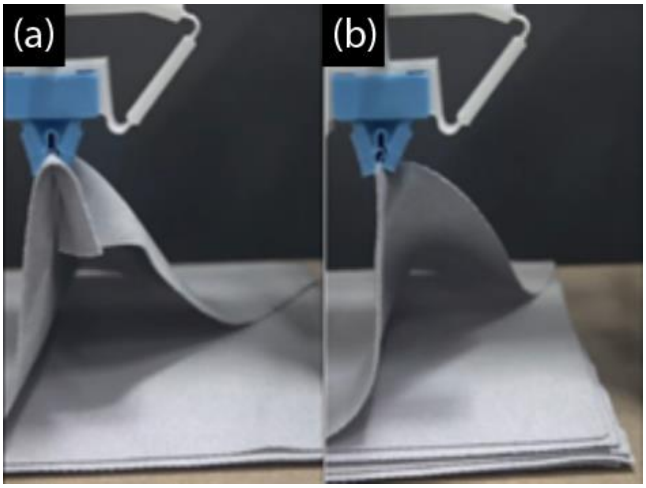

Figure 2.3: (a) Pinch gripping and (b) edge lifting.

2.2. Soft sensor design and working principle

Figure 2.4 shows the soft sensor and its working principle. The soft sensor comprises two conductive electrodes which are embedded into the gripping membrane. The electrodes are fabricated from a PDMS and carbon nanoparticle composite. The face of the electrodes facing away from the gripper are covered by a thin insulating layer, while the face of the electrodes facing the gripper are connected to wires which leave the gripper to an external circuit to provide sensor data. When the gripper is actuated, the electrodes face one another, acting as a parallel plate capacitor. The sensor's capacitance, ΔC, is dependent on the separation between the electrodes, d. Because the separation d is dependent on the number of fabric sheets gripped, by measuring the capacitance of the sensor, the number of fabric sheets gripped can be determined. Using equation 2.1, d can be calculated by the formula below:

$$d = \frac{\varepsilon_0 \varepsilon_r A}{2\Delta C} - t_m, \tag{2.1}$$

where ε_0 is the vacuum permittivity, ε_r is the dielectric constant, A is the area of the electrodes, and t_m is the thickness of the insulating layer covering the electrodes.

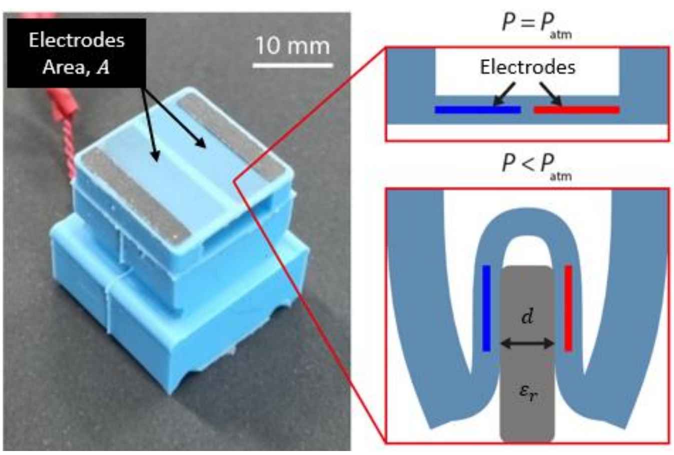

Figure 2.4: Soft sensor and soft sensor working principle.

To confirm the validity of equation (2.1) and the functionality of the soft sensor, a preliminary experiment was conducted by having the gripper grip different thicknesses of paper. The results of this preliminary experiment are shown in Figure 2.5, which show that the theory and experimental data are in well agreement.

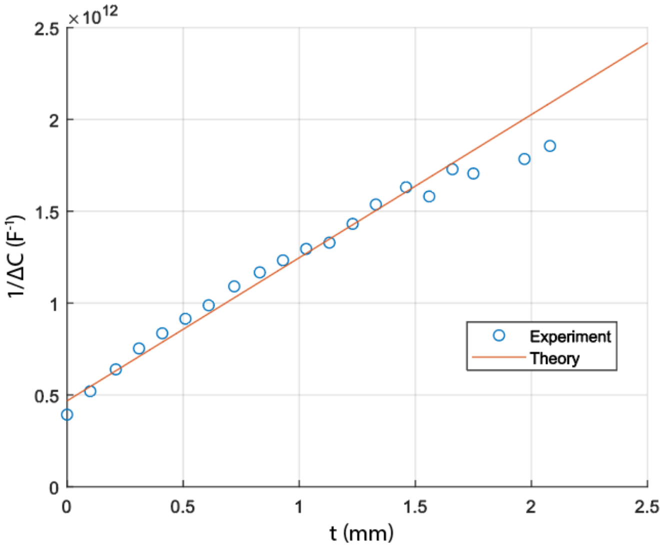

Figure 2.5: Sensor capacitance versus paper thickness. Experimental data is shown in blue circles. The solid line corresponds to the capacitance values predicted by theory.

Chapter 3. Gripper and Sensor Performance

3.1. Holding force

To quantify the gripping performance of the soft gripper, the holding force of the soft gripper was tested. As shown in Figure 3.1(a), the experimental setup comprises a custom-built normal force module, soft gripper, and a 50 mm by 100 mm fabric sample tethered to the worksurface with nylon string. Table 3.1 shows the 3 different types of fabrics used for the holding force experiment. The normal force module comprises a spring system, loadcell, pneumatic tubes and a gripper wrist. The loadcell records the force data during the experiment, and the gripper wrist acts as an adapter which houses the soft gripper while ensuring the gripper maintains the same orientation during contact with the fabric sample.

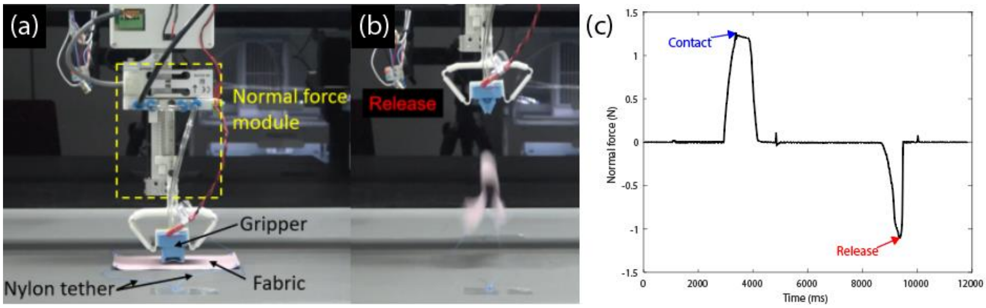

Figure 3.1: (a) Holding force experimental setup. (b) Snapshot of when gripper loses contact with fabric sample. (c) Force versus time data logged during one experimental trial.

Fabric	Thickness (mm)	Material	Air permeability (CFM)
I	0.08	Polyester	0.91
II	0.17	Polyester(90%), Spandex(10%)	0
III	0.27	Polyester	62.2

Table 3.1: Fabrics used to test the holding force of the soft gripper.

The experiment was conducted by having the gripper make contact with the fabric sample with a contact force of 1.25 N. This contact force was kept constant for all trials of the experiment. A vacuum was then applied to the gripper, actuating the gripper to grip the fabric sample. The level of vacuum applied was controlled with a digital air pressure regulator (SMC ITV2090). After actuation, the gripper was lifted slowly away from the worksurface. When the tension in the nylon tethers became too large for the gripper to maintain its grip on the fabric, the fabric was released from the gripper's grip as shown in Figure 3.1(b). The loadcell in the normal force module logged the force data during the experiment, and an example of the logged data is shown in Figure 3.1(c). From Figure 3.1(c), it is evident that the largest negative force is the total force the gripper can withstand before the grip on the fabric is lost. The holding force was therefore defined as the magnitude of the negative force.

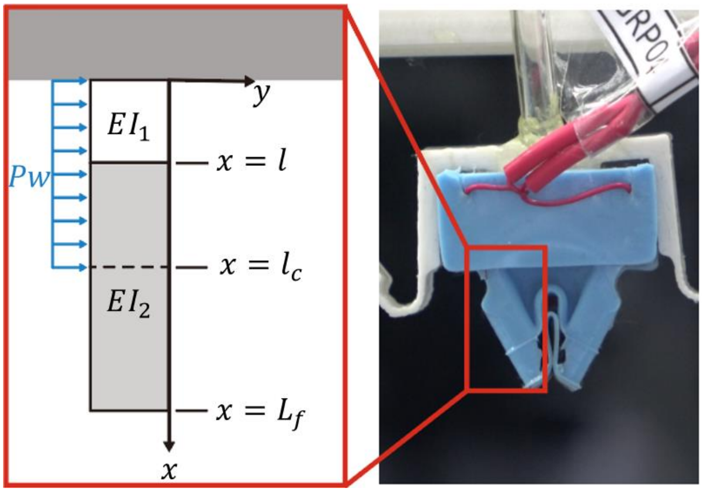

Figure 3.2: Schematic of the gripper beam model.

To provide a quantitative analysis of the holding force of the soft gripper, the gripping finger of the gripper was modelled as an elastic beam, as shown in Figure 3.2, where P is the vacuum pressure, w is the width of the gripping finger, EI_1 and EI_2 are the bending stiffnesses of the gripping finger notch and gripping finger, respectively. l, l_c, and L_f are the gripping finger notch length, cavity length, and total gripping finger length, respectively.

From Figure 3.2, it is clear that the beam can be divided into 3 regions due to discontinuities in bending stiffness and external forces. Using a similar approach employed by Kim and Mahadevan[9], in the region $0 < x < l$, where the gripping finger notch is located, $y = y_1(x)$ satisfies

$$EI_1 y_1''''(x) = Pw. \tag{3.1}$$

In the region $l < x < l_c$, where the cavity in which the vacuum acts, $y = y_2(x)$ satisfies

$$EI_2 y_2''''(x) = Pw. \tag{3.2}$$

In the region $l_c < x < L_f$, where the cavity in which the vacuum acts, $y = y_3(x)$ satisfies

$$y_3''''(x) = 0. \tag{3.3}$$

From equations (3.1) ~ (3.3), there are 12 constants of integration that need to be accounted for to provide a closed form solution. 8 constants of integration are accounted for with 8 matching conditions. At $x = l$ and $x = l_c$, the transverse deflection, slope, shear force and bending moments do not have any jumps. Therefore the following matching conditions can be applied:

$$\begin{aligned} y_1|_{x=l} &= y_2|_{x=l}, & y_2|_{x=l_c} &= y_3|_{x=l_c}, \\ y_1'|_{x=l} &= y_2'|_{x=l}, & y_2'|_{x=l_c} &= y_3'|_{x=l_c}, \\ y_1''|_{x=l} &= y_2''|_{x=l}, & y_2''|_{x=l_c} &= y_3''|_{x=l_c}, \\ y_1'''|_{x=l} &= y_2'''|_{x=l}, & y_2'''|_{x=l_c} &= y_3'''|_{x=l_c}. \end{aligned} \tag{3.4}$$

The remaining 4 constants of integration are accounted for with the boundary conditions. The boundary conditions depend on the magnitude of the vacuum pressure P. If the vacuum pressure P is small, the gripping fingers do not touch. In this case, the clamped beam condition can be applied at $x = 0$ and free end condition can be applied at $x = L_f$, leading to the following boundary conditions:

$$\begin{aligned} y_1|_{x=0} &= 0, & y_3''|_{x=L_f} &= 0, \\ y_1'|_{x=0} &= 0, & y_3'''|_{x=L_f} &= 0. \end{aligned} \tag{3.5}$$

As the magnitude of the vacuum pressure P is increased, eventually the gripping fingers will touch and apply a force against one another. As the free end boundary conditions no longer apply, another set of boundary conditions are required. Assuming symmetric actuation of the gripper, the displacement of the gripping fingertips should be half of the separation between the gripping fingers. Defining δ_m as half the separation of the gripping fingers, the following boundary conditions can be applied for this case:

$$y_1|_{x=0} = 0, \qquad y_3|_{x=L_f} = \delta_m,$$
$$y_1'|_{x=0} = 0, \qquad y_3''|_{x=L_f} = 0. \tag{3.6}$$

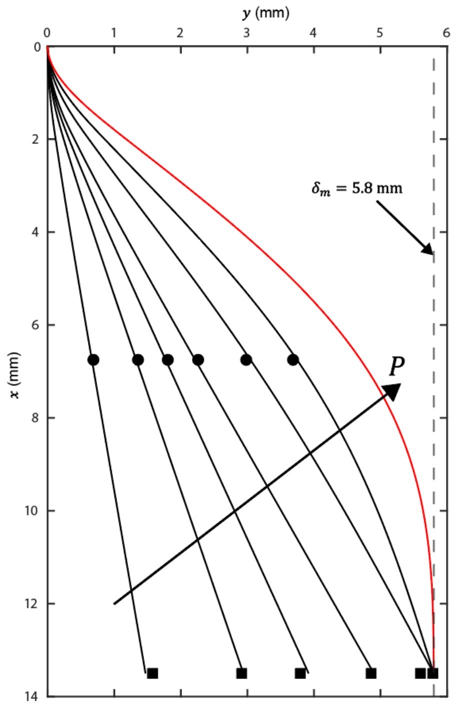

Figure 3.3: Deflection profiles of the gripping finger for varying vacuum pressure magnitudes. Solid lines are profiles obtained from solving equations (3.1) ~ (3.3). Black lines correspond to vacuum pressures of 3 kPa, 6 kPa, 8 kPa, 10 kPa, 30 kPa, and 60 kPa. The red line corresponds to a vacuum pressure of 101.325 kPa. The squares and circles denote experimentally obtained deflections for $x =$ 6.5 mm and $x =$ 13 mm, respectively. The grey dashed line is the maximum possible displacement of the gripping fingertip.

Figure 3.3 shows the deflection profiles for the gripping finger obtained for varying magnitudes of the vacuum pressure P. The boundary conditions (3.5) were used to obtain the deflection profiles for vacuum pressures below 11.9 kPa. For vacuum pressure above 11.9 kPa, the deflection of the gripping fingertips exceeds δ_m. Thus, for pressures exceeding 16.5 kPa, the boundary conditions (3.6) were used to calculate the gripping finger deflection profiles.

From Figure 3.3, it is clear that the beam model and experiments are in well agreement; therefore, the beam model can be used to provide a theoretical model for the holding force of the soft gripper. To calculate the holding force, $F_{\mathbf{hold}}$, the force the gripping fingertips push against each other with, F_n, needs to be calculated. From equations (3.1) ~ (3.3), matching conditions (3.4), and boundary conditions (3.6), F_n is

$$F_n = -EI_2 y_3'''(L_f). \tag{3.7}$$

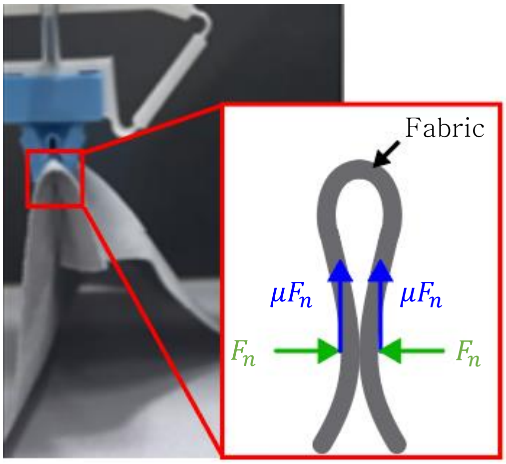

Figure 3.4: Photograph and free body diagram of fabric during grip.

Assuming that the holding force is friction dominated, the free body diagram of the fabric during grip is shown in Figure 3.4. Therefore, the holding force $F_{\mathbf{hold}}$ is calculated by the equation below:

$$F_{\mathbf{hold}} = 2\mu F_n, \tag{3.8}$$

where μ is the static coefficient of friction between fabric and silicone rubber. By setting $\mu = 1$[10], $F_{\mathbf{hold}}$ can now be calculated for a given vacuum pressure P.

The holding force calculated with equation (3.8) and the holding forces obtained experimentally with the fabrics from Table 3.1 are shown in Figure 3.5. Note that below the critical pressure of 11.9 kPa, the holding force calculated by the model is 0 N as the gripping fingers do not touch. When the vacuum pressure exceeds 11.9 kPa, the model predicts a linear relationship between holding force and vacuum pressure. The results of the experiments are in well agreement with the model until the vacuum pressure reaches 45 kPa. Beyond 45 kPa, the experimental data deviates from the model. A likely cause of this deviation is likely due to the limitations of Euler-Bernoulli beam theory which assumes small deformations and infinite depth; in the case of the soft gripper, the deformations are comparable to both the scale of the gripping finger length and the width. Thus, under high pressures, the theory may not fit well with experiments. Numerical methods may need to be employed to obtain exact solutions.

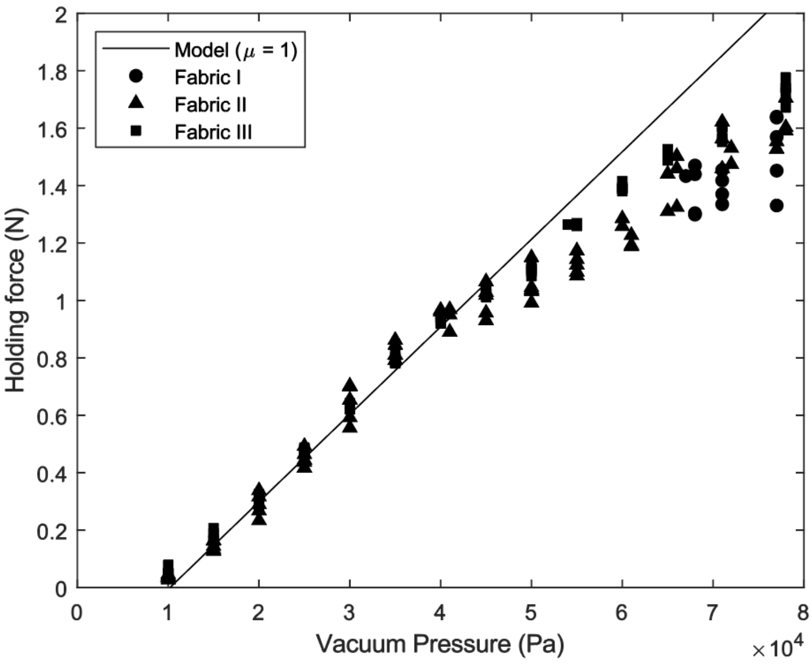

Figure 3.5: Holding force versus the magnitude of the vacuum pressure. The solid line represents the holding force calculated by equation (3.8). Experimentally obtained holding forces for different fabrics are shown as circles, triangles and squares.

3.2. Single ply gripping

For widespread adoption in the garments manufacturing industry, in addition to sufficient holding force for grip reliability, the ability to reliably grip a single sheet from a stack is extremely important, as garments manufacturing requires a precise quantity of specific fabrics for each manufacturing process. Therefore, the soft gripper's aptitude in reliably gripping single sheets of fabric is an important measure of the gripper's performance.

The single ply gripping reliability of the soft gripper was tested with 5 fabrics varying in thickness, material, and air permeability. The properties of the fabrics are shown in Table 3.2.

Fabric	Thickness (mm)	Material	Air permeability (CFM)
I	0.08	Polyester	0.91
II	0.17	Polyester (90%), Spandex (10%)	0
III	0.27	Polyester	62.2
IV	0.31	Nylon (69%), Polyester (31%)	0
V	0.44	Polyester	325

Table 3.2. Properties of fabrics used to test the soft gripper's single ply gripping capabilities.

To test the single ply gripping capabilities of the soft gripper, fabric sheets were cut into 225 cm^2 squares and were arranged into stacks of 350 sheets. The gripper then attempted to grip the fabric sheets from the stack. The contact force between the gripper and fabric stack was controlled to a constant 1.25 N. The results of the experiment are shown in Figure 3.6.

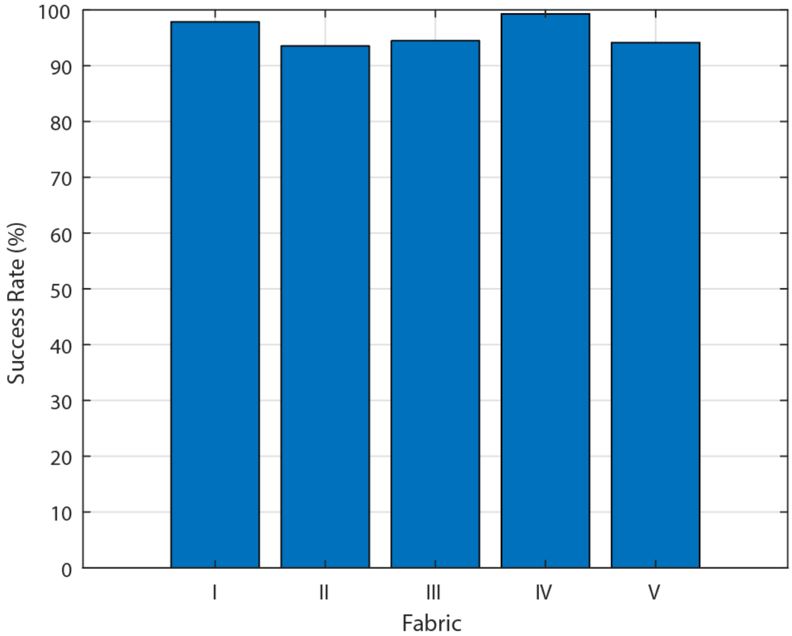

Figure 3.6: Single ply gripping performance of the soft gripper.

The soft gripper's grip success rate exceeded 90% for all fabric types, as shown in Figure 3.6. The lowest success rate was 93.55% for Fabric II and the highest success rate was 99.28% for Fabric IV. The mean success rate was 95.86%. The success rate only includes instances where the gripper gripped only a single sheet of fabric.

3.3. Sensing Performance

As outlined in Section 3.2, single sheet gripping is essential for applications in the garments manufacturing process. The soft sensor outlined in Section 2.2 allows the soft gripper to overcome instances when the gripper grips more than a single sheet of fabric or when the gripper is unable to grip a sheet of fabric by measuring the capacitance change upon gripper actuation.

The soft sensor's performance was measured through measuring the capacitance change of the soft sensor as the gripper gripped 0/1/2 layers of 5 different fabrics. The fabrics used are listed in Table 3.2. The results of the experiment are shown in Figure 3.7.

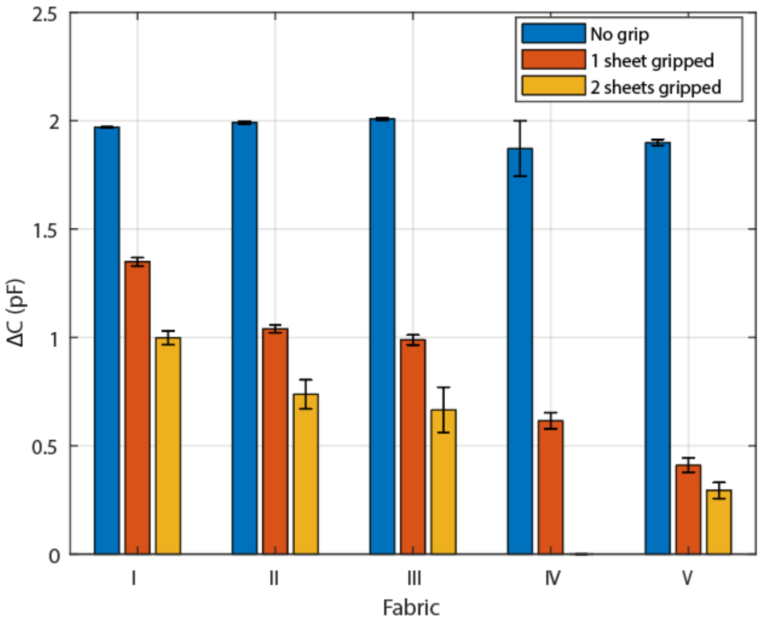

Figure 3.7: Soft sensor capacitance measurements for 5 different fabrics. Blue, orange and yellow bars correspond to capacitance changes when 0, 1 and 2 layers of fabric were gripped, respectively.

From Figure 3.7, there is a clear relationship between the number of fabric sheets gripped versus the capacitance change measured by the soft sensor: the higher the number of fabric sheets gripped, the lower the capacitance change registered. This is not surprising as the separation between the electrodes of the soft sensor increases with the number of fabric sheets gripped, lowering the capacitance of the soft sensor which acts as a parallel plate capacitor. Therefore, by measuring the capacitance change, the soft sensor is able to provide data from which the number of sheets of fabric can be deduced.

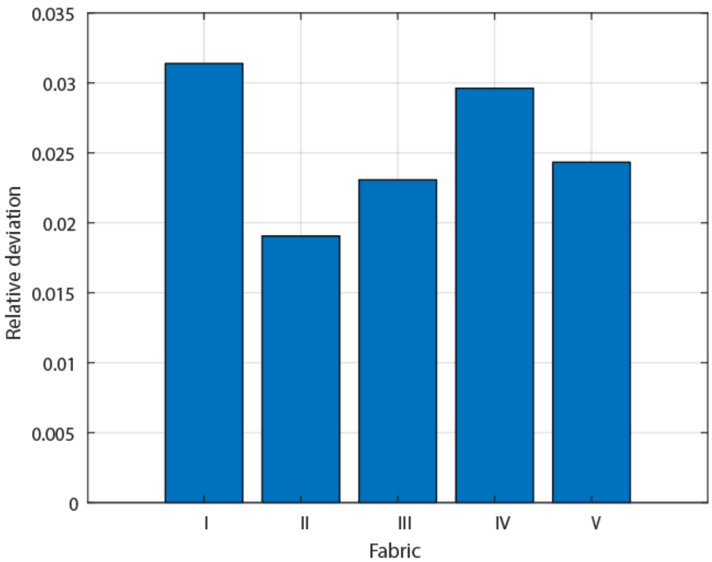

Figure 3.8: Relative deviation values for different fabric types.

From Figure 3.7, it is evident that the soft sensor’s performance is highly dependent on the type of fabric. To quantitatively assess the performance of the soft sensor for different fabric types, we define relative deviation, which can is calculated by the following formula:

$$\text{Relative deviation} = \frac{\sigma_1}{\Delta C_0 - \Delta C_1}, \tag{3.9}$$

where σ_1 is the standard deviation of the capacitance change when a single sheet of fabric is gripped, ΔC_0 is the mean capacitance change measured when no sheets of fabric are gripped, ΔC_1 is the mean capacitance change when a single sheet of fabric is gripped. σ_1 measures the repeatability of the soft sensor; a higher σ_1 means lower repeatability and therefore suggests low sensor performance. The denominator, $\Delta C_0 - \Delta C_1$, measures the sensitivity of the soft sensor; therefore, a larger value suggests higher sensor performance. A large relative deviation value, therefore, suggests low sensor performance. The relative deviations for each fabrics tested were calculated and plotted as shown in Figure 3.8. The soft sensor, according to relative deviation, had the best performance which Fabric II and the worst performance with Fabric I.

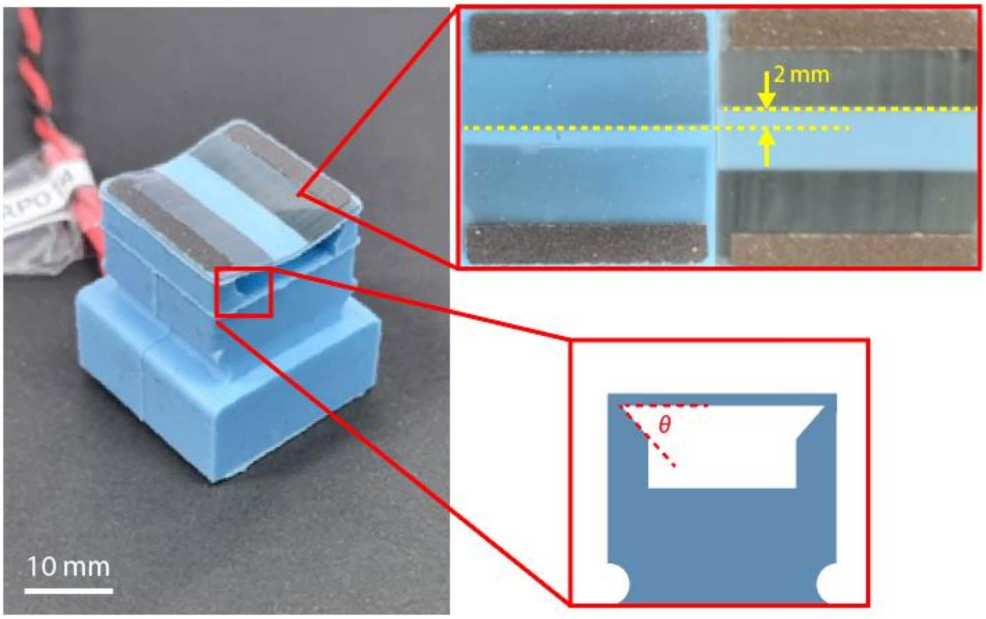

Figure 3.9: Changes made to the soft gripper and soft sensor for soft sensor performance optimization.

The performance of the soft sensor was further improved by making changes to the geometry of the soft sensor, as shown in Figure 3.9. The width of the soft sensor's electrodes was reduced by 2 mm to ensure that, during gripper actuation, the electrodes were solely separated by the gripped fabric. This reduced the capacitance contribution of the excess electrodes which were not separated by the gripped fabric.

The geometry of the soft gripper was also changed to optimize performance of the soft sensors. The gripping fingers' rectangular geometry causes the electrodes in the soft sensor to make line contact when the gripper is actuated, causing the electrodes to be separated by excessive and unnecessary empty space between the electrodes, decreasing sensor repeatability. Notches were added to the gripping fingers, as shown in Figure 3.9, to ensure a planar contact between the electrodes upon gripper actuation, ensuring that the electrodes are purely separated by fabric during gripping. The notch angle of 30° was obtained through iterative testing.

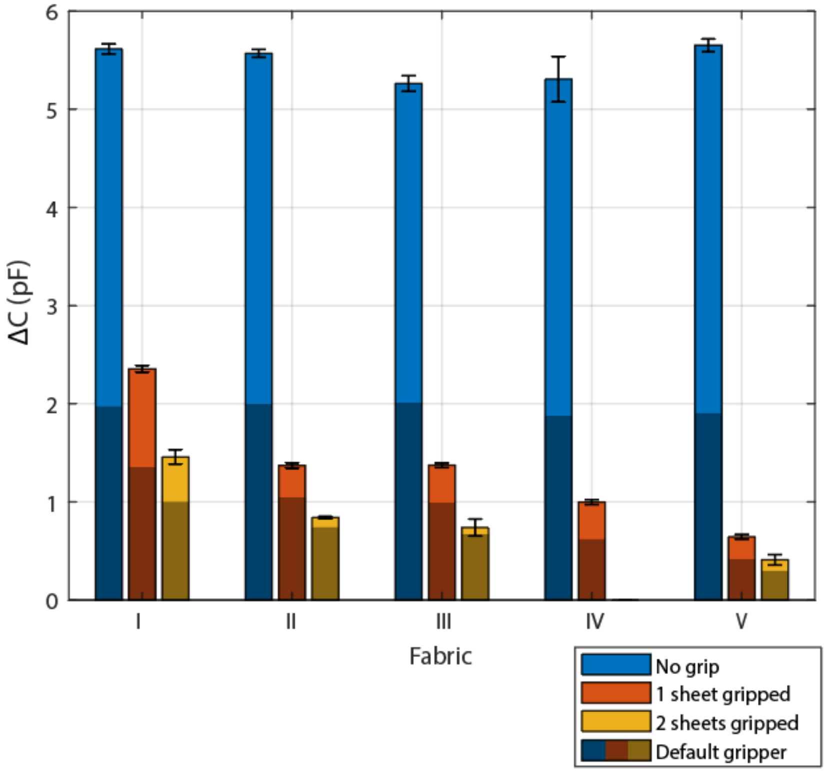

Figure 3.10: Improved soft sensor capacitance measurements for 5 different fabrics. Blue, orange, and yellow bars correspond to capacitance changes when 0, 1 and 2 layers of fabric were gripped, respectively. The darker bars correspond to the measurements taken by the soft sensor prior to the improvements.

The performance of the improved soft sensor was tested against the same fabrics listed in Table 3.2, and the results are shown in Figure 3.10. The blue, orange and yellow bars represent the capacitance change values measured by the improved soft sensor for 0 fabric sheets, 1 fabric sheet and 2 fabric sheets, respectively. The dark segments within the bars are capacitance levels measured by the soft sensor prior to the improvements. The modifications to the soft sensor and the soft gripper increase the capacitance change values for all five fabric samples, and clear differences in capacitance levels for different number of layers of fabric gripped implies good sensor functionality. To quantitatively assess whether the modifications have improved sensor functionality, the relative deviation of the modified soft sensor was calculated and plotted in Figure 3.11.

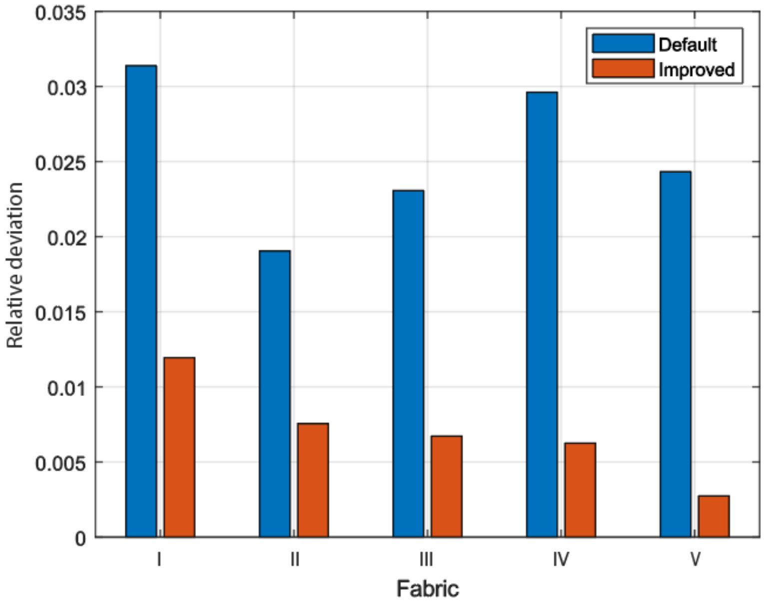

Figure 3.11: Relative deviation of the soft sensor prior (blue bars) and after (orange bars) modifying the soft sensor and gripper geometry.

From Figure 3.11, the relative deviation of the soft sensor's measurements have significantly decreased after modifying the sensor and gripper geometry, indicating a significant improvement to the sensor's performance. The improved soft sensor still performed the worst with Fabric I, as evidenced by the highest relative deviation, while performing the best with Fabric V.

The industrial application potential of the soft gripper and sensor were then explored with a simple pick-and-place task, as seen in Figure 3.12. When the gripper is unable to grip a sheet of fabric from a stack, as shown in Figure 3.12(a), the gripper approaches the fabric stack again to reattempt gripping a single fabric sheet from a stack. When more than one sheet of fabric is gripped, as shown in Figure

3.12(b) when two sheets were gripped, the gripper releases the fabric sheets back onto the stack and reattempts gripping a single sheet. As shown in Figure 3.12, the soft gripper and sensor were able to successfully determine cases where the number of fabric sheets gripped were not equal to one and reattempt the task until completed successfully.

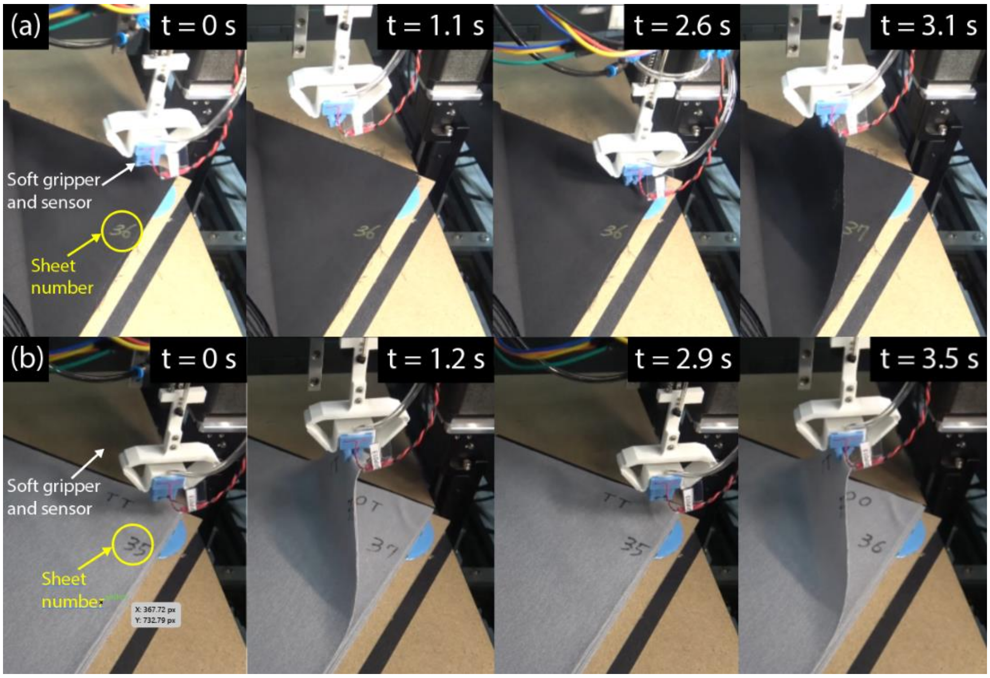

Figure 3.12: Pick-and-place application of the soft gripper and sensor. The soft gripper reattempts to grip a single sheet of fabric after gripping (a) no sheets and (b) 2 sheets of fabric.

Chapter 4. Conclusion

This thesis presented a soft gripper and soft sensor for extremely flexible objects, such as fabrics. The gripper comprises a cavity that, when exposed to a pneumatic vacuum, that collapses and pulls two gripping fingers in to grip the fabric sheet with a secure pinch. Though the soft gripper demonstrated a good single sheet gripping reliability for various types of fabric, a soft sensor was embedded into the gripper to compensate for the cases in which the gripper gripped 0 or more than one layer of fabric. The geometry of the soft gripper and electrodes in the soft sensor were then changed to optimize the performance of the soft sensor. The soft sensor and gripper were used to complete a pick-and-place task to demonstrate their industrial application potential.

Bibliography

[1] M. Bartosa, V. Bulej, M. Bohusika, J. Stanceka, V. Ivanov and P. Macek, An overview of robot applications in automotive industry, *Transportation Research Procedia* **55**, 837-844 (2021).

[2] S. Islam and S. T. S. Shazali, Determinants of manufacturing productivity: pilot study on labor-intensive industries, *International Journal of Productivity and Performance Management* **60**, 567-582 (2010).

[3] R. Kolluru, K. P. Valavanis, A. Steward and M. J. Sonnier, A flat-surface robotic gripper for handling limp material, *IEEE Robotics & Automation Magazine* **2**, 19-26 (1995).

[4] N. C. Tsourveloudis, R. Kolluru, K. P. Valavanis and D. Gracanin, Suction control of a robotic gripper: a neuro-fuzzy approach, *Journal of Intelligent and Robotic Systems* **27**, 215-235 (2000).

[5] G.J. Monkman, P.M. Taylor and G.J. Farnworth, Principles of electroadhesion in clothing robotics, *International Journal of Clothing Science and Technology* **1**, 14-20 (1989).

[6] P. M. Taylor, G. J. Monkman and G. E. Taylor, Electrostatic grippers for fabric handling, *Proceedings of the IEEE International Conference on Robotics and Automation*, 431-433 (1988).

[7] Market available Needle Grippers, www.eoat.net, from ATS Automation Technology Schwope Inc., Germany.

[8] Market available Needle Grippers, www.vmeca.com, from VMECA Co., Ltd., South Korea.

[9] H.-Y. Kim and L. Mahadevan, Capillary rise between elastic sheets, *Journal of Fluid Mechanics* **548**, 141-150 (2006).

[10] S. Ku, J. Myeong, H.-Y. Kim, and Y.-L. Park, Delicate fabric handling using a soft robotic gripper with embedded microneedles, *IEEE Robotics and Automation Letters* **5**, 4852-4858 (2020).

Abstract in Korean

초유연 물체용 소프트 센서와 그리퍼

서울대학교 대학원

기계공학부

안 우 상

본 연구에서는 원단과 같은 초유연 물체용 소프트 센서와 그리퍼를 개발하였다. 소프트 그리퍼는 내부 캐비티, 캐비티 벽, 그리핑 핑거, 그리핑 막으로 구성되어 있다. 내부 캐비티에 압력 강하를 가할시 그리핑 핑거가 오므라지면서 원단을 집는 그리핑 방식을 사용한다. 소프트 그리퍼의 원단 그리핑 성능 평가하기 위해서, 다양한 원단 상대로 소프트 그리퍼의 그리핑 힘과 낱장 그리핑 성공률을 시험 평가했다. 그리고 원단 두께 측정을 통해서 그리핑된 원단 개수 판별 가능한 소프트 원단 센서를 개발하고 다양한 원단 상대로 소프트 센서의 원단 낱장 판별 성능 시험 평가 및 분석했다. 그리고 소프트 그리퍼와 소프트 센서 성능 최적화 하였다.

주요어: 소프트 그리퍼, 소프트 센서, 자동화

학 번: 2019-21912